

Improving MF R-Mode ranging performance with measurement-based correction factors

1st Filippo Giacomo Rizzi
German Aerospace Center (DLR)
Neustrelitz, Germany
Filippo.Rizzi@dlr.de

2nd Niklas Hehenkamp
German Aerospace Center (DLR)
Neustrelitz, Germany
Niklas.Hehenkamp@dlr.de

3rd Lars Grundhöfer
German Aerospace Center (DLR)
Neustrelitz, Germany
Lars.Grundhoefer@dlr.de

4th Stefan Gewies
German Aerospace Center (DLR)
Neustrelitz, Germany
Stefan.Gewies@dlr.de

Abstract—The advent of global satellite navigation systems (GNSS) has revolutionized the provision of position, navigation and timing (PNT) information. Thought to be always available and reliable, these systems may experience outages and they can be threatened by interference events. In such cases, alternative positioning, navigation and timing (APNT) systems play a key role. In the maritime domain Ranging Mode, called R-Mode, is a rising terrestrial alternative to GNSS. R-Mode exploits medium frequency (MF) signals transmitted by maritime radio beacons in one possible implementation. It is well-known that MF radio waves are affected by attenuation and distortion caused by a change in the electrical properties of the ground along the propagation path. Additionally, terrain elevation variation and large metallic infrastructures introduce further distortions in the signal, decreasing the overall ranging performance. In this paper we propose a novel approach to compensate for this effect based on direct range measurements. The theory is explained in depth and a test case, based on real measurement campaign data, to validate the technique is also presented.

Index Terms—APNT, R-Mode, MF correction

I. INTRODUCTION

Nowadays, global navigation satellite systems (GNSS) are the primary source of position, navigation and timing (PNT) information in the maritime domain. Nevertheless, in the last decades, the threats to GNSS receivers have been rapidly increasing, highlighting the necessity of alternatives and backup systems for navigation [1, 2]. Furthermore, system errors and outages can cause unavailability or, more dangerously, misleading information. This is a serious threat for shipping.

Ranging Mode (R-Mode) is an innovative terrestrial navigation system under development [3]–[5]. Based on the signal of opportunity (SoOP) concept, the system reuses maritime radio beacons to broadcast synchronized ranging signals in the maritime medium frequency (MF) band around 300 KHz [6]. Additionally, the system can use the maritime VHF infrastructure [7, 8], with signals transmitted at around 162 MHz, but that is not the focus of this paper. Therefore, for the rest of this paper when the expression R-Mode is used, we always refer to the MF part of the system.

Ranging information, representing the distance between the transmitter and the receiver, is obtained by measuring the phases of sinusoidal components of the R-Mode signal [9].

Medium frequency signals propagate as ground wave that follows the curvature of the Earth and is therefore not restricted to the line-of-sight (LOS) limitation. This propagation mode is due to the large conductivity of the ground in the frequency band which results in a guiding-wave mechanism for medium and low frequencies [10, 11]. The typical radio beacon service reach is about 250 kilometers in distance. During the propagation from the transmitter to the ship, the signal passes different areas with different electrical properties. This means the propagation starts on land, where the transmitter is located, and changes after some kilometers to a sea path before it is received by a maritime user. The propagation path can be even more complicated with a number of sections of sea and land. Unfortunately, each section causes a ground-dependent change of the propagation speed [12] with respect to the vacuum, which introduces a delay to the signal which has to be known to compute accurate ranging and positioning with MF R-Mode.

The most important parameter for compensating such a delay is the ground conductivity which represents the electrical conductivity of the earth's surface. In the literature, the signal attenuation and delay for a single position and a given transmitter can be calculated with the help of Millington's method [13] and the information of the electrical ground conductivity for all homogenous sections of the propagation path between transmitter and receiver. In general, over sea water the conductivity remains reasonably constant, therefore the introduced delay is easier to compensate. Because the ground conductivity of land depends on soil type, soil water content, acidity, and temperature, the true value is mostly unknown. This makes predictions of the correction parameter inaccurate and reduces the performance. For MF R-Mode we defined as Atmospheric and Ground wave propagation Delay Factor (AGDF) the predicted signal delay based on the knowledge of the atmospheric parameters and the ground conductivity maps.

Most often only rough ground conductivity maps exist [14].

When using these for the generation of AGDF maps, this helps to reduce the ranging error in an R-Mode receiver but significant errors remain. Additionally, a delay may also be introduced by the variation in the terrain elevation along the path, resulting in a longer travelled distance. Lastly, large metallic infrastructures, such as bridges or power line plants, can produce a further signal distortion which is complex to be modelled [15].

In order to compensate for the aforementioned additional biases and modelling mismatch, one solution is to exploit direct measurements in the field. This second approach enhances the prediction quality, as it will be shown. In this paper we show the impact of unmodelled delay sources and propose a novel methodology to generate a correction function dependent on the azimuth which improves the ranging accuracy.

The paper is divided as follows: Sec. II briefly describes the theory on the AGDF. In Sec. III the new methodology is illustrated in detail, with the description of the main assumptions and validity of the technique. In Sec. IV we apply the proposed approach on real data from a measurement campaign, presenting the achieved improvement with respect to the application of AGDF alone. Finally, Sec. V concludes the paper.

II. ATMOSPHERIC AND GROUND WAVE DELAY FACTOR

When a ground wave travels along a finitely conducting surface, it experiences a complex attenuation which causes a damping of amplitude and a phase delay [11]. The effect can be described by an attenuation function that accounts for ground wave-related effects with respect to free-space propagation. By using the ground conductivity, permittivity and distance travelled as input values, the argument of the attenuation function provides the negative phase delay of the wave with respect to vacuum free space propagation. To correct phase estimates which are used for ranging in R-Mode and determine pseudoranges using the vacuum speed of light, the phase delay can simply be added to the measurement. On a non-homogeneous, segmented propagation path with sections of different electrical properties, the argument of the attenuation function of each segment can be concatenated by using the Millington/Pressey [12] method to obtain the phase delay of that mixed path. The phase delay added to the distorted phase estimate serves as the so-called AGDF for R-Mode.

To obtain the AGDF for an arbitrary propagation path, the paths composition has to be determined. Since the ITU World Atlas of Ground Conductivities [14] provides a database of electrical properties for a large portion of the earth, it can be used to determine the composition by extracting the ground conductivity and distance from segments of equal conductivity along the propagation path from the transmitter to the receiver. For each segment, the attenuation function is calculated using the well-known method introduced by Rotheram [16, 17] and Wait [11] before concatenating the functions of all segments using the Millington/Presseys method. The solution provided by Rotheram's approach accounts not only for the finite

conductivity of a curved earth surface but also for refraction in the exponential atmosphere.

In comparison to Loran-C [15], a terrestrial low frequency navigation system which today is only available in a few parts of the world, the AGDF represents the sum of primary, secondary and additional secondary factors. In the case of the AGDF, the effects that are modelled with the primary and secondary factors are not computed separately or approximated through polynomials.

Fig. 1 provides an example of the AGDF calculated with the ITU-R Ground Conductivity maps for a transmitter located next to Groß Mohrdorf in the north of Germany. The introduced phase delay compared to propagation in vacuum is given here in radians. By observing the gradient in the color map it is clear that the right side area of the transmitter is affected by a different delay compared to the left side. In particular, a higher delay is expected on the right part due to the presence of additional land (the island of Rügen), which causes a reduction in the propagation speed with respect to the sea.

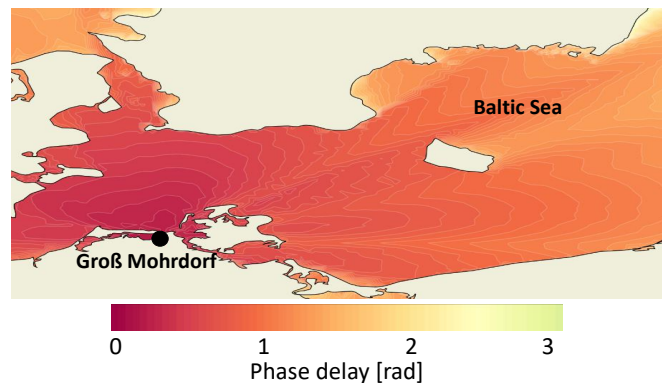


Fig. 1. Groß Mohrdorf AGDF calculated for the southern Baltic Sea in radians.

The accuracy of the correction obtained with the described approach depends strongly on the quality of the ground conductivity maps utilized. If the conductivity value in the maps closely represent reality, the estimated signal delay will be accurate. Unfortunately, the ground conductivity data is quite old and, in general, with low spatial resolution.

Additionally, this approach does not include a model to compensate for the delay introduced by the variation in the terrain elevation. Also, distortion generated by metallic infrastructures, which may be encountered by the signal along the propagation path, are not incorporated. Therefore, to overcome these limitations and increase the ranging accuracy, the approach described in the next section, based on direct-range measurements, has been established and evaluated.

III. GENERATING A DIRECT MEASUREMENT-BASED CORRECTION FUNCTION

In this section we describe how to exploit R-Mode pseudorange measurements in combination with GNSS based ranges to produce a correction function which increases the R-Mode ranging accuracy. MF R-Mode pseudorange measurements are

computed by using phase observation derived from transmitted pilot sinusoidal signals. The concept is similar to the GNSS carrier phase observation and the interested reader can refer to [9] for a detailed explanation of the MF R-Mode ranging and positioning principles. The phase variation between transmitter and receiver is equivalent to the travelling time of the signal and therefore the pseudorange ρ_R in meters can be expressed as follows:

$$\rho_R = c(t_{rx} - t_{tx}) \quad (1)$$

with c the propagation speed in vacuum and t_{rx} , t_{tx} are reception and transmission time respectively. To be precise, phase observations are ambiguous due to the cyclic nature of the sinusoidal signal and a single cycle has an equivalent distance of approximately 1 km. Therefore, an important task of the receiver is the resolution of such an ambiguity. At the time of writing, the DLR software receiver solves the ambiguity by performing an initial calibration process which uses GNSS data, as explained in [9].

As discussed previously, different impairments affect the signal along its path, hence the pseudorange model can be expressed as follows

$$\rho_R = d + b_{CK} + b_{AGD} + b_{TE} + b_O + n \quad (2)$$

with d the geodesic distance between receiver and transmitter, modelled with the Vincenty's formula [18], b_{CK} the combined receiver and transmitter clock offset, b_{AGD} the delay induced by the atmosphere and ground wave propagation as explained in Sec. II. The terrain elevation error is represented by b_{TE} whereas the unmodelled distortions, due to large ferromagnetic obstacles, are described by b_O . Last but not least, n is a noise term which depends on the receiver itself and the received signal-to-noise (SNR) ratio. With the help of a GNSS receiver, which provides accurate information about the position of the vessel, the transmitter-receiver distance can also be easily calculated and we define the GNSS range as follows

$$\rho_G = d + n' \quad (3)$$

where n' represents the noise in the range which depends on the working mode of the GNSS receiver and its internal algorithms, going from a few meters for single point positioning (SPP) to a few centimeters for real-time kinematic (RTK) or precise point positioning (PPP).

We define the difference between R-Mode and GNSS range as

$$\Delta\rho = \rho_R - \rho_G \quad (4)$$

and by substituting (2) and (3) in (4) we obtain

$$\Delta\rho = b_{CK} + b_{AGD} + b_{TE} + b_O + n'' \quad (5)$$

with $n'' = n - n'$. It is clear that $\Delta\rho$ represents a noisy version of the delay budget. By using a receiver which is synchronized with the transmitters, the clock bias can be neglected, hence $b_{CK} \approx 0$. Additionally, even in a non-synchronized scenario this could also be estimated and removed by using transmitter clock offset data correction, which will be broadcast by the

service provider and from the positioning, velocity and timing (PVT) algorithm of the R-Mode receiver.

We can now apply a filter to remove the noise term n'' . Different filtering strategies can be applied but for this paper a simple average window forward-backward filtering has been considered. The filtered delay budget, $\Delta\rho_f$, can then be represented as follows

$$\Delta\rho_f = b_{AGD} + b_{TE} + b_O \quad (6)$$

as a clean version of the delay components.

In principle, if the ground conductivity maps used for the prediction coincide with the real ground conductivity, the bias b_{AGD} can be removed completely. Nevertheless, due to the mismatch between real and assumed values a residual bias remains, which we define as

$$b_{AGD_r} = b_{AGDF} - b_{AGD} \quad (7)$$

where b_{AGDF} represents the predicted correction obtained as explained in Sec. II. We then define the overall residual error, which we call Model Error (ME), since it accounts for model mismatch and unknown or unmodelled source of delay (b_{AGD_r} , b_{TE} and b_A), as follows

$$b_{ME} = b_{AGDF} - \Delta\rho_f = b_{AGD_r} - b_{TE} - b_O \quad (8)$$

Finally, a function $f_{ME}(\alpha)$ based on the azimuth angle α (angle formed by the vector connecting the transmitter and the vessel and the transmitter vector pointing to the north) is generated. Such a function can be easily obtained by using interpolation or fitting techniques. In this work a cubic 1D interpolator has been used.

To clarify the principle of this methodology, we use Fig. 2 to provide a simple explanation to the reader. Suppose the transmitter is located on an island depicted by the gray circle area, the main assumption is that the majority of the delay introduced in the signal is due to the land component of the path. Indeed, on this section we have higher variability of the ground conductivity, terrain elevation and potential additional source of distortion. The assumption is that a measurement has been taken on the point P_1 (yellow cross), which has an arbitrary azimuth α . By applying the described process from (4) to (8), one can obtain the ME for that azimuth. Imagine now performing a second measurement on P_2 (red cross) which is located at a longer distance from the transmitter but with the same azimuth angle α of P_1 . Assuming that the ground conductivity maps are accurate on the sea path section, the variation due to the land component should in principle be the same as for P_1 . Therefore, the ME computed for P_1 is also applicable to P_2 .

This description should clarify the overall procedure to compute and apply the proposed correction scheme. With this approach we try to capture high-order biases introduced in the signal mainly by the land path section between the transmitter and the coast. Therefore, its main limitation is the assumption that no additional land path is encountered between the coast and the vessel. Nevertheless, even in this case the correction

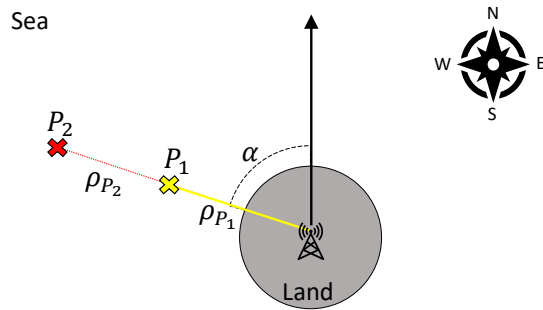


Fig. 2. Explanation for generating the correction function.

still holds, but it cannot include compensation for the additional ground area which must be then compensated separately. The main advantage of this approach is that, in principle, by only surveying the entire azimuth on the sea once we can apply the correction over a large and extensive maritime area. This clearly reduces not only the effort of planning and conducting measurements on a large area, but also drastically decreases the cost of the survey campaigns.

IV. APPLICATION AND RESULTS

To showcase the validity of the suggested approach, the algorithm was applied in post-processing on real data gathered during a measurement campaign conducted on 20th February 2021. The ship Deneb was equipped with an MF R-Mode receiver built by the German Aerospace Center capable of providing not only ranges but also positioning [9]. The receiver was combined with an accurate rubidium clock in order to perform research activities avoiding synchronization issues, therefore in this case the assumption of synchronized receiver and transmitter is valid and the term b_{CK} is neglected. Moreover, a GNSS receiver with RTK grade positioning performance was used to obtain a reference trajectory which was used to derive accurate ranges as in (3).

Fig. 3 presents the map of the considered case scenario. The Groß Mohrdorf transmitter, which is the one under study, is visible as a yellow triangle. Two trajectories are also visible, the blue one, indicated as forward path, has been used to generate the ME correction function. Here the vessel was sailing from the shore towards the Baltic Sea. Whereas the red dashed route, named backward path, since the vessel was sailing back towards the coast, has been used to validate the approach.

In Fig. 4 two curves related to the forward path are presented. The difference between the R-Mode range and the GNSS one in blue ($\Delta\rho$) and the predicted AGDF with the red dotted line (b_{AGDF}). Both of them are given in meters and obtained with 1 Hz measurements. It appears clear that the AGDF provides corrections which follow the general trend of the introduced bias. This means that, in general, the ground conductivity maps are suitable for correcting large errors. Nevertheless, as discussed in Sec. II, it does not model all the types

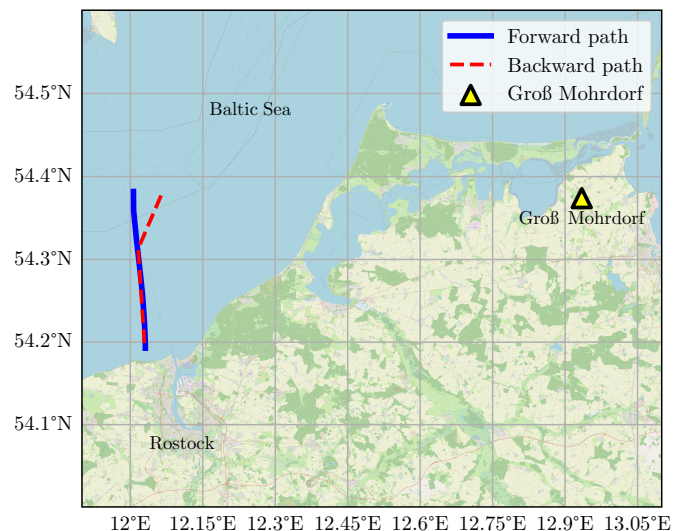


Fig. 3. Map showing the test scenario. The yellow triangle represents the Groß Mohrdorf transmitter location, the blue line is the forward path (shore to sea) whereas the red dashed line shows the backward path (sea to shore).

of variations accurately due to the maps mismatching and the possible additional error sources. Therefore, in such a case a residual error will remain reducing the overall performance of the system. The difference between the two curves describes the existence of the error which remains uncorrected in the range.

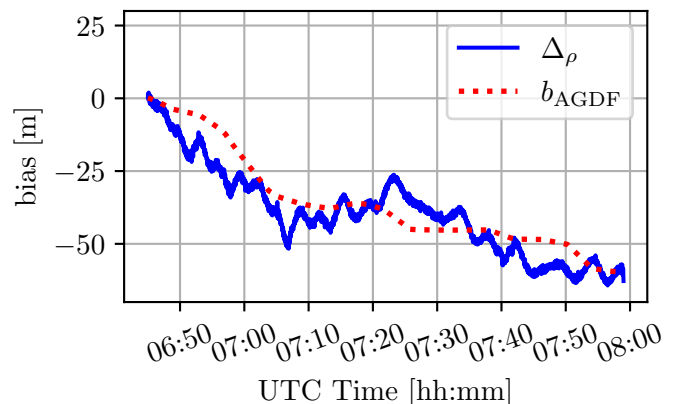


Fig. 4. Comparison between true range error $\Delta\rho$ (blue line) and AGDF prediction (red dotted) in meters.

After applying a 30s window averaging in a forward-backward mode on $\Delta\rho$ to cancel out the noise, we can use (8) to obtain the high correction term b_{ME} . This is plotted in Fig. 5 as a function of the azimuth angle. The negative azimuth values are justified by the fact that they are defined in the range $(-180, 180]$ northwards. As a last step to derive the correction function $f_{ME}(\alpha)$, the points are interpolated by using a cubic interpolator algorithm.

The obtained function can now be used to predict the signal delay with higher accuracy. The function was tested to predict

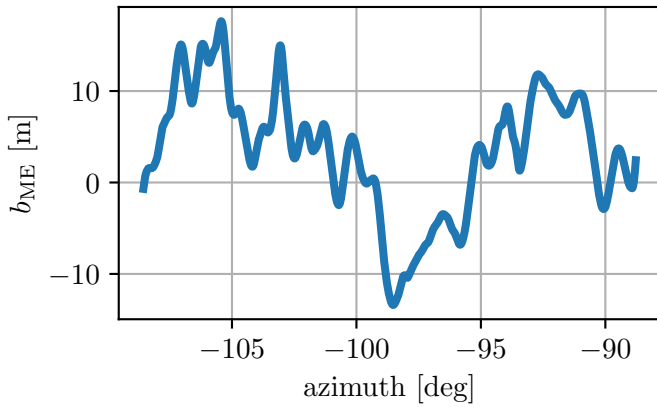


Fig. 5. Residual model error (ME) in meters in function of the azimuth computed for the forward path.

the corrections on the backward path which is characterized by similar values of azimuth as can be deduced from Fig. 3. On top of the AGDF correction, we therefore apply the correction derived from the ME function.

The density histograms in Fig. 6 represent the absolute value of the error on the R-Mode range for two cases: The blue histogram is obtained when only the AGDF is used, whereas the orange histogram is produced when the ME function is used in combination with the AGDF (AGDF+ME). The improvement is clearly visible. In fact, we can see how the orange distribution is closer to zero. The range error significantly decreases when the ME function is used. In particular, the maximum absolute error goes from 18.4 m to 10.9 m while the 95% error is reduced from 13.9 m to 7.8 m.

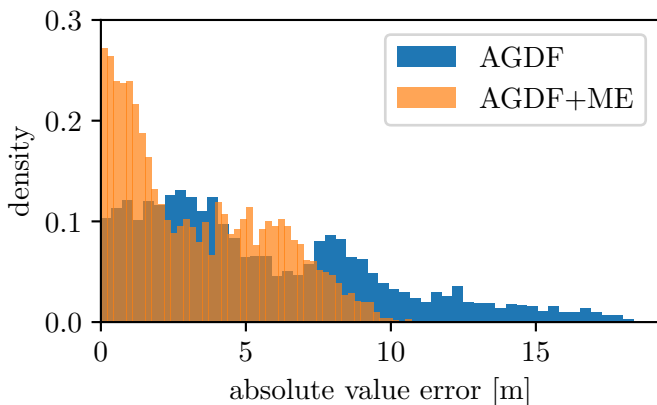


Fig. 6. Density histogram of the absolute value range error: AGDF in blue and AGDF+ME in orange.

The improvement of the range accuracy achieved with the proposed methodology is an essential step to meet navigational requirements in the maritime domain. Such requirements for backup navigation systems are listed in the IALA recommendation R-129 [19], and in particular R-Mode aims in providing its navigational services in coastal areas, where

the horizontal accuracy required is 100 m (95%) and in port, restricted waters and inland waterways, where 10 m (95%) is necessary. Nevertheless, it is important to remember that the horizontal positioning accuracy does not only depend on the range accuracy. In fact, the geometry represented by the transmitter and receiver locations, often referred to as horizontal dilution of precision (HDOP), also plays a fundamental role in determining the final covariance matrix and accuracy of the positioning solution. Thus, good ranging accuracy combined with good HDOP (< 2) are necessary conditions to meet the requirements.

V. CONCLUSION

In this paper we proposed an innovative approach to increase the accuracy of the MF R-Mode ranging exploiting direct in-field measurements and GNSS positioning information. After briefly describing the source of error and the way in which current corrections are generated, the new proposed methodology was explained in depth. A test case was presented in order to show that the method can provide improvements with respect to the sole use of AGDF based on ground conductivity maps. In the presented scenario the absolute range error was evaluated and its 95% value decreased from 13.9 m to 7.8 m when AGDF was combined with the use of ME correction. This level of improvement opens the door to the usability of the system where the 10 m horizontal positioning accuracy needs to be met.

The main advantage of the suggested technique remains in the fact that only small-scale measurement campaigns are needed to characterize the signal delay, generating a correction function dependent only on the azimuth angle. In principle, only one-way path survey covering all the azimuth angles from the transmitter would be sufficient, therefore the cost and the time of the survey campaign can be remarkably reduced. Nevertheless, the assumption of no additional land between the coast line and the point of application must be fulfilled in order to obtain accurate ranging. If this is not the case, the correction can still be applied but with an expected reduced accuracy.

Improving the quality of the AGDF maps might be seen as an alternative way to enhance the accuracy of the system. This different approach would be optimal, allowing to use well-know prediction formulas but has two main challenges. First of all, the generation of high accuracy maps requires a deep and consuming surveying campaign. Secondly, some differences between the estimated value and the reality might remain due to local effects which are of extreme complexity to be modelled.

Future activities aim to extensively validate the approach by performing additional survey campaigns analysing the proposed methodology to verify its potential performance and limits of applicability thoroughly. The results shown in this paper are of particular interest for the national maritime service providers since we demonstrated that the MF signal delay can be directly measured and therefore, a correction service can be then established, so that the provider can broadcast additional

correction information to the user to improve the overall R-Mode service quality.

ACKNOWLEDGMENT

The research was conducted in the framework of the R-Mode Baltic 2 project which aims to perform a long-time evaluation of the R-Mode performance and to test new R-Mode concepts to improve the R-Mode performance and independence from GNSS. The authors thank Saab AB (publ) TransponderTech and the entire R-Mode Baltic 2 project team and especially our partners Gutec AB and the German Federal Maritime and Hydrographic Agency for their support in the preparation and conduction of the sea trials. Furthermore, the authors thank the European Union for co-financing the R-Mode Baltic 2 project through the European Regional Development Fund within the Interreg Baltic Sea Region Programme.

REFERENCES

- [1] J. A. Volpe, "Vulnerability assessment of the transportation infrastructure relying on the Global Positioning System," Volpe National Transportation Systems Center, Tech. Rep., 2001.
- [2] T. R. A. o. Engineering, *Global Navigation Space Systems: reliance and vulnerabilities*, March 2011.
- [3] S. Gewies, A. Dammann, R. Ziebold *et al.*, "R-Mode testbed in the Baltic Sea," in *19th IALA Conference*, Incheon, Republic of Korea, 2018.
- [4] G. Johnson, K. Dykstra, S. Ordell, and P. Swaszek, "R-mode positioning system demonstration," in *Proceedings ION GNSS+ 2020*. ION, september 2020.
- [5] J. Šafář, A. Grant, P. Williams, and N. Ward, "Performance Bounds for VDES R-Mode," *Journal of Navigation*, vol. 73, pp. 92 – 114, 2019.
- [6] G. Johnson and P. Swaszek, "Feasibility study of R-Mode using MF DGPS Transmissions," ACCSEAS Project, Tech. Rep., 2014c.
- [7] —, "Feasibility study of R-Mode using AIS transmissions: Investigation of possible methods to implement a precise GNSS independent timing signal for AIS transmission," ACCSEAS Project, Tech. Rep., 2014b.
- [8] M. Wirsing, A. Damman, and R. Raulefs, "VDES R-Mode performance analysis and experimental results," in *International Journal of Satellite Communications and Networking*, 2021, pp. 1–20.
- [9] L. Grundhöfer, F. G. Rizzi, S. Gewies *et al.*, "Positioning with medium frequency R-Mode," *Navigation*, vol. 68, p. 829–841, 2021.
- [10] International Telecommunication Union, "Handbook on ground wave propagation," 2014.
- [11] J. R. Wait, "The ancient and modern history of em ground-wave propagation," *IEEE Antennas and Propagation Magazine*, vol. 40, no. 5, pp. 7–24, 1998.
- [12] B. G. Pressey, G. E. Ashwell, and F. C. S., "The measurement of the phase velocity of ground-wave propagation at low frequencies over a land path," in *Proceedings of the IEE - Part III: Radio and Communication Engineering*, March 1953, p. 73 – 84.
- [13] G. Millington, "Ground-wave propagation over an inhomogeneous smooth earth," *Journal of the Institution of Electrical Engineers*, vol. 96, pp. 53–64, 1949.
- [14] International Telecommunication Union, *ITU-R P.832-4 World atlas of ground conductivities*, Geneva, July 2015.
- [15] U.S. Coast Guard, *Loran-C User Handbook*, April 1992.
- [16] S. Rotheram, "Ground-wave propagation. part 1: Theory for short distances," in *IEE Proceedings F-Communications, Radar and Signal Processing*, vol. 128, no. 5. IET, 1981, pp. 275–284.
- [17] —, "Ground-wave propagation. Part 2: Theory for medium and long distances and reference propagation curves," *IEE Proceedings F Communications, Radar and Signal Processing*, vol. 128, no. 5, p. 285, 1981.
- [18] T. Vincenty, "Direct and inverse solutions of the geodesics on the ellipsoid with application of nested equations," *Survey Review*, vol. 23, no. 176, pp. 88–93, Apr 1975.
- [19] IALA, *Recommendation R-129 on GNSS vulnerability and mitigation measures*, 3rd ed., December 2012.